#### **European Journal of Soil Science**

European Journal of Soil Science, Volume 65, Issue 2, Pages 248–263, March 2014



### Assessment of soil organic carbon at local scale with spiked NIR calibrations: effects of selection and extra-weighting on the spiking subset

Journal:	European Journal of Soil Science
Manuscript ID:	EJSS-060-13.R1
Manuscript Type:	Original Manuscript
Date Submitted by the Author:	24-Aug-2013
Complete List of Authors:	Guerrero, César; Universidad Miguel Hernandez de Elche, Agroquímica y Medio Ambiente Stenberg, Bo; Swedish University of Agricultural Sciences, Soil and Environment Wetterlind, Johanna; SLU, Department of Soil and Environment Viscarra Rossel, Raphael; CSIRO, Land and Water Maestre, Fernando; Universidad Rey Juan Carlos, Departamento de Biología y Geología Mouazen, Abdul Mounem; National Soil Science Institute, Natural Resources Department Zornoza, Raul; Universidad Politécnica de Cartagena, Departamento de Ciencia y Tecnología Agraria Ruiz-Sinoga, Jose Damian; Universidad de Málaga, Departamento de Geografía Kuang, Boyan; Cranfield University, Natural Resources Department
Keywords:	SOC assessment, soil sensing, near infrared spectroscopy, spiking, extra- weighting

SCHOLARONE<sup>™</sup> Manuscripts

Published by Wiley. This is the Author Accepted Manuscript.

This article may be used for personal use only. The final published version (version of record) is available online at 10.1111/ejss.12129. Please refer to any applicable publisher terms of use.

1	Assessment of soil organic carbon at local scale with spiked NIR
2	calibrations: effects of selection and extra-weighting on the spiking
3	subset
4	C. GUERRERO <sup>A</sup> , B. STENBERG <sup>B</sup> , J. WETTERLIND <sup>B</sup> , R.A. VISCARRA ROSSEL <sup>C</sup> , F.T.
5	MAESTRE <sup>D</sup> , A.M. MOUAZEN <sup>E</sup> , R. ZORNOZA <sup>F</sup> , J.D. RUIZ-SINOGA <sup>G</sup> & B. KUANG <sup>E</sup>
6	<sup>a</sup> Departamento de Agroquímica y Medio Ambiente, Universidad Miguel Hernández de
7	Elche, E-03202, Spain, <sup>b</sup> Department of Soil and Environment, SLU, Skara, Sweden,
8	<sup>c</sup> CSIRO Land and Water, Canberra, Australia, <sup>d</sup> Departamento de Biología y Geología,
9	Universidad Rey Juan Carlos, Spain, <sup>e</sup> Department of Environmental Science and
10	technology, Cranfield University, UK, <sup>f</sup> Departamento de Ciencia y Tecnología Agraria,
11	Universidad Politécnica de Cartagena, Spain, and <sup>g</sup> Departamento de Geografía,
12	Universidad de Málaga, Spain.
13	Correspondence: César Guerrero. E-mail: <u>cesar.guerrero@umh.es</u>
14	Running title: Spiking and extra-weighting to improve soil organic carbon predictions
15	with NIR
16	
17	

#### 19 Summary

Spiking is a useful approach to improve the accuracy of regional or national 20 spectroscopic calibrations when they are used to predict at local scales. To do this, a 21 small subset of local samples (spiking subset) is added to recalibrate the regional or 22 national calibration. If the spiking subset is small in comparison with the size of the 23 initial calibration set, then the spiking subset could have little noticeable effect and only 24 a small improvement can be expected. For these reasons, we hypothesised that the 25 accuracy of the spiked calibrations can be improved when the statistical relevance of the 26 27 spiking subset is given extra-weight. We also hypothesised that the spiking subset selection and the initial calibration size were relevant, and could affect the accuracy of 28 the recalibrated models. To test these hypotheses, we evaluated different strategies to 29 select the best spiking subset, with and without extra-weighting, to spike three initial 30 calibrations of different sizes. These calibrations were used to predict the soil organic 31 carbon (SOC) content in samples from four target sites. Our results confirmed that 32 spiking improved the prediction accuracy of the initial calibrations. We observed 33 differences in accuracy depending on the spiking subset used. The best results were 34 35 obtained when the spiking subset contained local samples evenly distributed in the 36 spectral space, regardless of the initial calibration's characteristics. The accuracy was significantly improved when the spiking subset was extra-weighted. For medium- and 37 large-sized initial calibrations, the improvement due to extra-weighting was larger than 38 that caused by the increase in spiking subset size. This result is interesting because 39 extra-weighting the spiking subset is an inexpensive task. Similar accuracies were 40 obtained using small- and large-sized initial calibrations, suggesting that incipient 41 spectral libraries could be useful if the spiking subset is properly selected and extra-42 weighted. When small-sized spiking subsets were used, the predictions results were 43

#### **European Journal of Soil Science**

44 more accurate than those obtained with 'geographically local' models. Overall, our results indicate that we can minimise the efforts needed to effectively use near-infrared 45 (NIR) spectroscopy for SOC assessment at local scales. 46

47

48

Keywords: SOC assessment, soil sensing, near infrared spectroscopy, spiking, extra-weighting. 49

50

#### Introduction 51

Using near-infrared (NIR) spectroscopy to estimate soil properties is rapid, non-52 destructive and relatively inexpensive compared to conventional laboratory analyses, 53 54 particularly when processing many samples. For NIR spectra to be quantitatively useful, we need to develop and use a soil spectral database or library to derive spectroscopic 55 models (calibrations) that relate the spectra to analytical data, e.g. soil organic carbon 56 (SOC). When assessing soil properties at a local scale, we can develop site-specific or 57 'geographically local' calibrations (Wetterlind *et al.*, 2010) that are generally very 58 59 accurate because smaller areas tend to be less variable in terms of the dependent 60 variable (Stenberg et al., 2010), and the samples used to develop the calibration and 61 those used for prediction share similar characteristics, such as mineralogy and organic matter quality (Reeves et al., 1999; Janik et al., 2007; Guerrero et al., 2010; Wetterlind 62 et al., 2010). A disadvantage of these models is that they are only valid for the local 63 area, which could be an expensive strategy when evaluating multiple areas. Another 64 option is to use regional, national or global calibrations, but they should represent the 65 variability of the soils being analysed. This has caused a trend to develop larger-scale 66 calibrations with a very large number of samples to ensure that the local samples fall 67

68 within the model's domain (Shepherd & Walsh, 2002; Brown et al., 2006; Viscarra Rossel, 2009; Grinand et al., 2012; Viscarra Rossel & Webster, 2012), although this 69 cannot be guaranteed because soils have such variable characteristics, even at a regional 70 scale. Furthermore, a set of samples comprising a large-scale calibration should be 71 considered heterogeneous, but the local samples could be considered as a homogeneous 72 set that is located in a small area of the overall calibration domain. This could be the 73 reason for inaccurate (biased) results observed by some authors when using regional 74 75 and national calibrations to make predictions at local scales (Brown et al., 2005; Brown, 2007; Janik et al., 2007; Christy, 2008; Sankey et al., 2008; Guerrero et al., 2010; 76 Stenberg et al., 2010; Wetterlind & Stenberg, 2010), even when the local samples fall 77 within the model domain and are not recognised as outliers. This could also explain 78 why better results are obtained with local (spectrum-specific) models (Genot et al., 79 2011; Gogé et al., 2012), where a subset of library samples that are similar to the 80 unknown sample is used to construct the calibration (Pérez-Marín et al., 2007). 81 However, local methods are expensive because a large spectral library is needed to find 82 sufficient similar samples for the calibrations. 83

Spiking is an alternative method proposed to improve the accuracy of regional or 84 national calibrations for use at local scales (Viscarra Rossel et al., 2009; Guerrero et al., 85 86 2010; Stenberg et al., 2010; Wetterlind & Stenberg, 2010; Kuang & Mouazen, 2013). Spiking—sometimes referred to as 'augmentation' (Brown *et al.*, 2006; Brown, 2007; 87 88 Sankey et al., 2008) and other names—involves three main steps (Janik et al., 2007). First, analyse a few samples from the target site in the laboratory using the reference 89 method; then add these samples to the initial calibration matrix; and then recalibrate the 90 model. This procedure usually increases the accuracy of the predictions in the rest of the 91 samples from the target site (Brown et al., 2005; Sankey et al., 2008; Wetterlind & 92

93 Stenberg, 2010). The higher the number of local samples in the spiking subset, the higher the accuracy in the prediction set (Brown, 2007; Guerrero et al., 2010), but a 94 large spiking subset decreases the advantages of NIR spectroscopy as a quick and low-95 cost analytical method. To increase the relative proportion of the spiking subset, 96 Guerrero et al. (2010) suggested decreasing the number of samples in the initial 97 calibration set because they obtained higher accuracies when small-sized calibrations 98 99 were spiked, where the spiking subset had a larger influence. However, the selection of 100 a small number of calibration samples can reduce the amount of important information 101 for modelling, and lead to less robust calibrations. For this reason, we proposed an alternative approach to increase the relevance of the spiking subset in the NIR 102 calibrations. The approach is to increase the statistical weight of the spiking subset by 103 adding several copies of the subset to the calibration matrix. These extra-weighted 104 samples are more important than other samples used to form the statistical model 105 (Capron et al. 2005; Stork & Kowalski 1999), which forces the calibration to better fit 106 the extra-weighted samples. If these samples were similar to the overall prediction set, 107 the model should provide more accurate predictions. We also evaluated different 108 strategies to select the best spiking subset. Since each local sample is different to the 109 others, we hypothesised that the selection of a spiking subset would influence the 110 111 accuracy of the spiked models, and the selection would be more influential if fewer samples were used for spiking. 112

The spiking approach tries to gain benefits from a previously developed or initial large-scale calibration set. It is reasonable to assume that results obtained could be affected by the characteristics of the initial calibration, as some authors observed (Guerrero *et al.*, 2010; Wetterlind & Stenberg, 2010). For this reason, we included different initial calibrations in this study and evaluated their influence on the spiking

118 process. Our first objective was to evaluate how local samples should be selected as a spiking subset for optimal spiking. To do this, we compared thirteen different strategies 119 to select the samples for the spiking subset. Our second objective was to evaluate 120 whether an extra-weighted spiking subset increased the prediction accuracy. In addition, 121 we compared geographically local models that used three different sized spiking 122 subsets. We selected SOC as the soil property for prediction, and we used the 123 coefficient of determination  $(R^2)$ , root mean square error of prediction (RMSEP). 124 standard error of prediction (SEP) and ratio of performance to deviance (RPD) to 125 evaluate the prediction performance for four different target sites. 126

#### 127 **2. Material and methods**

#### 128 2.1. National samples and initial calibrations

A national soil library (n = 2836) of soils from different sites across Spain 129 (predominantly southeastern Spain) was randomly split into three subsets. These subsets 130 were used to create three initial calibrations of different sizes, representing three 131 different stages or efforts to develop the spectral library: small (IC#1; n = 192), medium 132 133 (IC#2; n = 365) and large (IC#3; n = 2279). The soils in the soil library were collected 134 under forest and agricultural land uses. Most of these soils developed over sedimentary 135 (mostly calcareous) lithologies. The soil samples were air-dried and sieved ( $\leq 2 \text{ mm}$ ), and the NIR spectra (12 000-3800 cm<sup>-1</sup>) were obtained by FT-NIR diffuse reflectance 136 spectroscopy (MPA, Bruker Optik GmbH, Germany). The scale of the spectra was 137 transformed to nanometers (830-2630 nm), and re-sampled to 1 nm resolution. The 138 SOC concentration (%) was determined using the Walkley & Black (1934) method. The 139 different initial calibrations, relating the SOC to the NIR spectra, were constructed 140

- 141 using partial least squares (PLS) regression (PLS-1 algorithm) (see section 2.6 for
- 142 details). Key characteristics of the initial calibrations are shown in Table 1.

143 2.2. Target sites

We selected four independent target sites from four regions with spectral characteristics 144 145 that differed from each other and from those observed in the initial calibrations (Figure 1; Appendix 1). Each target site is a relatively small area of dense sampling, 146 from several hectares to a few square kilometres in size. A different number of local 147 samples were collected at each target site (Table 2). One site was located in Sweden 148 149 (TS1), two in Spain (TS2, TS3) and one in the United Kingdom (TS4). As with the initial calibration samples, the soil samples from the target sites were air-dried and 150 sieved (< 2 mm), and the NIR spectra and SOC content were obtained. Most of the 151 spectra were collected using a FT-NIR (MPA, Bruker Optik GmbH, Germany), except 152 the TS1 samples, which were scanned using a vis-NIR (ASD FieldSpec Pro Fr, USA). 153 The scale of the FT-NIR spectra was transformed from cm<sup>-1</sup> to nanometers, and re-154 sampled to 1 nm. For details about FT-NIR and vis-NIR scanning, see Guerrero et al. 155 (2010) and Wetterlind & Stenberg (2010), respectively. 156

157 2.3. Calibration types

Different types of calibrations relating SOC and NIR spectra were obtained using PLS as a regression method (see section 2.6), and were used to predict the SOC contents in the target site samples.

161 Initial calibrations: three different-sized initial calibrations (IC#1, IC#2 and IC#3,

- described in section 2.1) that did not contain any samples from the target sites;
- referred to as unspiked initial calibrations (Figure 2a; section 2.6).

Spiked calibrations: the three initial calibrations modified by adding a spiking subset
(n = 8) (Figure 2b). We used 13 different spiking subsets to spike each of the initial
calibrations (see section 2.4). In each initial calibration, we obtained 13 subtypes of
spiked calibrations, and we repeated this procedure for each of the four target sites.
Spiked calibrations with extra-weighting: in each of the different spiked calibrations,
the spiking subset was extra-weighted. To do this, we added 24 copies of each
spiking subset sample to the calibration set (Figure 2c), and then recalibrated the

model (see section 2.6). Each of the eight spiking subset samples appears 25 times

in the calibration matrix, becoming 24 times more influential than the soil library

samples because we have modified their leverage (Stork & Kowalski, 1999). We

selected 24 copies because the leverage of the target site samples followed an

asymptotic pattern after the addition of 15–20 copies (data not shown).

#### 176 2.4. Strategies to select the spiking subset from the target site samples

171

172

173

174

175

177 For each target site, we used 13 strategies to select the different types of spiking subsets. 178 We hypothesised that each strategy had different advantages. The strategies were 179 designed and grouped on the basis of (i) the SOC values of target site samples, (ii) the spectral characteristics of the target site samples and (iii) the spectral relationships 180 between the initial calibrations and the target site samples using the Mahalanobis 181 182 distance values. The first group of five strategies was designed on the basis of the SOC content of target site samples. These strategies have a strictly theoretical value for 183 interpreting some results because the SOC contents of the target site samples would be 184 unknown in a real scenario, and thus these strategies would not be useful in practice. 185

186 Strategy 1 (OC low): select eight target site samples with the lowest SOC values (left
187 tail of SOC histogram). Samples with low SOC contents will show more clearly the

### **European Journal of Soil Science**

188	spectral features of the inorganic constituents, which are the most important factors
189	impeding the use of a calibration from one site to another. Moreover, these samples
190	could be useful to correct the bias in target site samples with low SOC contents.
191	Strategy 2 (OC high): select eight target site samples with the highest SOC values (right
192	tail of SOC histogram). These samples mask the inorganic spectral features, and
193	clearly show the SOC spectral features in the local samples. Moreover, these
194	samples can be useful to correct bias in target site samples with high SOC contents.
195	Strategy 3 (OC tails): select four samples with the lowest SOC values (from the left tail
196	of the SOC histogram) and four with the highest SOC values (from the right tail).
197	These samples can be useful to correct bias because the low and high SOC contents
198	are well established. Since low and high values are well described, the offset should
199	be also corrected.
200	Strategy 4 (OC centre): select eight target site samples with SOC values around the
201	median SOC value of the set.
202	Strategy 5 (OC distrib): select eight target site samples at regular intervals over the
203	entire range of SOC values (samples evenly distributed across the SOC values).
204	These samples should also be adequate for bias and offset correction.
205	To apply the three strategies in the second group, we performed a principal
206	component analysis (PCA) of the target site samples (NIR spectra pre-processed with
207	Savitzsky-Golay first derivative). The scores of the first, second and third principal
208	components (i.e. the first three) are represented in a scatter-plot.
209	Strategy 6 (PC periph): select eight target site samples located at the periphery of the
210	principal component spectral space defined by the first three principal components.

#### **European Journal of Soil Science**

211 Strategy 7 (PC centre): select eight target site samples located at the centre of the principal component spectral space defined by the first three principal components. 212 These are the most similar samples to the mean spectrum of the target site spectra. 213 Strategy 8 (PC distrib): select eight target site samples evenly distributed across the 214 215 principal component spectral space defined by the first three principal components. This is the most intuitive strategy to uniformly cover the spectral diversity. This 216 217 selection was made using the 'Automatic selection subset' option in OPUS (version 6.5 software; BrukerOptik GmbH, Ettlingen, Germany), which selects 218 samples in a similar fashion to the Kennard–Stone algorithm (Kennard & Stone, 219 1969). 220 The third group of five strategies was based on the Mahalanobis distance values of 221 the target site samples. The Mahalanobis distance values were calculated with respect to 222 223 the unspiked initial calibrations. Each target site sample had a different Mahalanobis 224 distance depending on the initial calibration used (i.e. IC#1, IC#2 or IC#3). Strategy 9 (MD low): select eight target site samples with the lowest Mahalanobis 225 226 distance values (left tail of Mahalanobis distance histogram). These target site samples are the closest to the initial calibration samples and the overall target site 227 samples, and could become a 'bridge' between both sets. 228 Strategy 10 (MD high): select eight target site samples with the highest Mahalanobis 229 distance values (right tail of Mahalanobis distance histogram). These samples are 230 the first recognised as outliers. In some schemes of calibration maintenance 231 (Shepherd & Walsh; 2002), it has been suggested the addition of this type of 232 samples when calibrations must be updated. These target site samples are the most 233 effective decreasing the Mahalanobis distance of the overall target site set (Capron 234 235 et al., 2005).

Strategy 11 (MD tails): select four target site samples with the lowest Mahalanobis
values and four with the highest Mahalanobis distance values.

- Strategy 12 (MD centre): select eight target site samples with Mahalanobis distance
  values around the median Mahalanobis distance value.
- Strategy 13 (MD distrib): select eight target site samples at regular intervals over the
  entire range of Mahalanobis distance values (samples evenly distributed across the
  Mahalanobis distance values).

#### 243 2.5 Experimental design and statistical analysis

For this study, a repeated measures factorial design was established. The between-244 245 subject factors were 'initial calibration', with three levels (i.e. three initial calibrations 246 of different sizes, IC#1, IC#2 and IC#3) and 'strategy', with 13 levels (i.e. 13 spiking subset selection strategies). The within-subject factor was 'extra-weighting', with two 247 levels (i.e. without and with extra-weighting). For each combination of factors, we 248 calculated the  $R^2$ , RMSEP, SEP and RPD to compare the actual SOC content of the 249 target site samples with the SOC predicted by the different calibrations. This design was 250 applied separately to the four target sites. The prediction performance parameters 251 obtained in each target site were considered as replicates. We used RMSEP to inform us 252 253 about accuracy and SEP about precision. The RPD (the ratio between the standard deviation of the prediction set and the RMSEP) allowed us to compare the accuracy 254 obtained in prediction sets with different standard deviations. 255

The differences in RMSEP, SEP and RPD were analysed using a repeated measures ANOVA. We excluded the strategies based on the SOC values (strategies 1–5) from the statistical analysis because they are not useful in practice. In this way, the repeated measures ANOVA was performed using eight levels of spiking subset selection strategy

260 and three levels of initial calibration as the between-subject factors, and two levels of extra-weighting as the within-subject factor. Homocedasticity and normality was 261 checked using Levene and Kolmogorov-Smirnov tests, respectively; the original 262 variables were transformed to meet with the ANOVA assumptions when appropriate. 263 The  $R^2$  was excluded from this statistical analysis because it did not meet the 264 assumptions. The assumption of sphericity was not violated when using the Mauchly's 265 test of sphericity. The software IBM SPSS Statistics version 20 (IBM, Armonk, NY) 266 267 was used for statistical analyses. We also obtained predictions using the unspiked initial 268 calibrations, but these results were not included in the statistical analysis.

#### 269 2.6. Development of calibrations with PLS-regression

The models relating the NIR spectra with the SOC contents in soils were obtained with 270 PLS-regression (PLS-1 algorithm; OPUS version 6.5 software; BrukerOptik GmbH, 271 Ettlingen, Germany). We selected the number of PLS-vectors through leave-one-out 272 cross-validation. Before calibration, the SOC contents were transformed by the square 273 root but predicted SOC data were back-transformed before we compared them with 274 actual SOC and calculated the prediction performance parameters. NIR-spectra were 275 transformed by the first derivative (Savitzsky–Golay, 25 points). The number of PLS-276 277 vectors in the spiked calibrations was set to the same number as in the corresponding initial calibration. In TS1, we used the spectral range 1000–2500 nm to meet a common 278 range with a similar noise to the spectra collected with the FT-NIR instrument. 279

# 2.7. Additional comparisons: extra-weighting effect versus the increase of the spiking subsets size and versus geographically local models

These comparisons were made only with spiking subsets selected by the 'PC distrib' strategy, which was one of the most effective selection strategies in terms of increasing

accuracy. We compared the extra-weighting effect against the increase of the spiking 284 subsets size. To do this, we spiked the three initial calibrations with 8, 16 and 285 32 spiking subset samples selected by the 'PC distrib' strategy. Similar to the procedure 286 described in section 2.3, we obtained spiked calibrations by adding 24 copies of the 287 spiking subset (denoted as EW 24). For each target site, we used these calibrations to 288 predict the SOC contents in the target site samples. In all cases, the 32 spiking subset 289 290 samples were not used in the RMSEP computation, to allow a fair comparison of 291 accuracy regardless of the size of the spiking subset. The RMSEP values were analysed with a repeated measures ANOVA, where two levels of extra-weighting (with and 292 without extra-weighted) acted as the within-subject factor, and three levels of the 293 spiking subsets size (8, 16 and 32 samples) acted as the between-subject factor. Due to 294 the large differences between the sizes of the initial calibrations, we also used a 295 different approach to calculate the number of copies to add, which was the ratio 296 between the initial calibration size and the spiking subset size. In this way, more copies 297 are added when the initial calibration size is larger or when the spiking subset size is 298 smaller. The extra-weighting effect obtained using the initial calibration-to-spiking 299 subset ratio (denoted as EW ratio) was evaluated using repeated measures ANOVA, as 300 for the EW 24 approach. The data used in these statistical analyses did not violate the 301 302 ANOVA assumptions (homocedasticity and normality) or the condition of sphericity. For each target site, three geographically local or site-specific models were constructed 303 304 using the 8, 16 and 32 spiking subsets selected by the 'PC distrib' strategy.

305 **3. Results** 

#### 306 *3.1. Effect of spiking (without extra-weighted)*

307 The predictions obtained with the unspiked initial calibrations for each target site were inaccurate, with large prediction errors (Figure 3). For the 12 cases (three initial 308 calibrations applied to four target sites), the RPD values ranged from < 0.10 to 1.44, 309 which clearly indicated poor predictions. Figure 4 shows the  $R^2$ , RMSEP, SEP and RPD 310 values obtained with the unspiked and spiked calibrations, where each value shown is 311 the mean value of those obtained for the four target sites. The unspiked IC#1 provided 312 very low quality predictions, with  $R^2 = 0.33 \pm 0.34$  (mean  $\pm$  standard deviation) and 313  $RPD = 0.52 \pm 0.21$  (Figure 4a). Once spiked, we observed a drastic and positive change 314 315 in all the parameters related to the quality of predictions (Figure 4a), and bias was substantially decreased. There were differences in accuracy for the spiked calibrations 316 depending on the strategy used to select the spiking subset. For example, the RMSEP 317 values obtained with the IC#1 spiked using the 'OC low'(worst) and 'PC distrib'(best) 318 strategies were  $0.70 \pm 0.16\%$  and  $0.37 \pm 0.15\%$  SOC, respectively, both of which were 319 clearly better than the RMSEP for the unspiked IC#1 of  $1.86 \pm 1.77\%$  SOC (Figure 4a). 320 Similarly, spiking of IC#2 (Figure 4b) caused a noticeable improvement in prediction 321 accuracy, mostly due to improvement of bias. Interestingly, the worst ('OC low') and 322 best ('PC distrib') strategies for IC#2 were the same as those observed for IC#1. A 323 substantial improvement in accuracy was also obtained when IC#3 was spiked, due to a 324 325 strong decrease in bias (Figure 4c). In this case, the worst and best strategies (in terms of accuracy) were not the same as for IC#1 and IC#2. In general, the best accuracies 326 327 were obtained using IC#1 (the calibration with the smallest size) and the worst accuracies were obtained with IC#3 (the calibration with the largest size). To illustrate 328 the effect of spiking with different spiking subsets, individual results for the four target 329 sites obtained with the 'MD centre' and 'PC distrib' selection strategies are shown in 330 Figure 3. 331

332 *3.2. Effect of extra-weighting on the spiking subset selection strategies* 

The addition of several copies of the spiking subset (i.e. extra-weighting) in the spiked calibrations caused a significant improvement (P < 0.001) in the RMSEP, SEP and RPD (Table 3). The effect of extra-weighting on these parameters was similar across the spiking subset selection strategies (extra-weighting × strategy, P > 0.05; Table 3), and also similar in the three different initial calibrations evaluated (extra-weighting × initial calibration, P > 0.05; Table 3), although the extra-weighting effect on the  $R^2$  was greater in IC#3 (Figure 4).

We observed that accuracy differed depending on the strategy used to select the 340 spiking subset (Figure 4). Indeed, all the parameters evaluated showed significant 341 differences across the strategies (Table 3). The differences between strategies were 342 similar in the three initial calibrations evaluated, as suggested by the non-significant 343 interaction between the 'strategy' and the 'initial calibration' (P > 0.05; Table 3). In two 344 345 strategies ('OC low' and 'OC high'), extra-weighting had a negative effect through an increase in bias (Figure 4). The 'OC low' strategy was worst for IC#2 and IC#3, and 346 second worst for IC#1. When extra-weighting was applied, 'PC distrib' was the best 347 348 performing strategy in the three initial calibrations, and clearly improved the accuracy 349 due to decrease in bias, but also due to a decrease in SEP (Figure 3 & Figure 4). In IC#1 and IC#2, the combined use of the spiking subset ('PC distrib') and extra-weighting 350 increased the RPD by 1.5 units compared to the unspiked initial calibrations, allowing 351 352 RPD values to exceed 2 (Figure 4). The results obtained with the 'MD centre' and 'PC distrib' strategies (without and with extra-weighting) for each target site illustrate the 353 354 extra-weighting effects (Figure 3).

3.5. *Increase of spiking subsets size versus extra-weighting, and comparison with* 3.5. *geographically local models* 

357 We compared the effects of increasing the spiking subset size with extra-weighting for the 'PC distrib' selection strategy. There was a positive effect on the accuracy when the 358 spiking subset size was increased (Figure 5), although this effect was not significant 359 (P > 0.05; Table 4). Regardless of the spiking subset size, there was a significant 360 improvement in the accuracy when the spiking subsets were extra-weighted (P < 0.001, 361 Table 4). These results were similar for the two approaches followed to select the 362 number of copies to add for extra-weighted (Table 4, Figure 5). It is worth highlighting 363 364 that in IC#2 and IC#3, the improvement of the accuracy due to extra-weighting was 365 clearly higher than the duplication of the spiking subset size (Figure 5), and even higher than the quadruplication of the spiking subset size in IC#3 (Figure 5). The extra-366 weighting effect in IC#1 was smaller because spiking was enough to cause the 367 saturation of the improvement, mainly due to it smaller size. When the spiking subset 368 was not extra-weighted (black bars in Figure 5), the best results were obtained with the 369 small-sized initial calibration (IC#1), and results obtained with IC#2 and IC#3 were less 370 accurate than those obtained with the geographically local models. Once the spiking 371 subset was extra-weighted, the differences between initial calibrations practically 372 disappeared, especially when the number of copies added was selected according to the 373 ratio of the initial calibration to the spiking subset (EW ratio; light grey bars in 374 375 Figure 5). When this approach was used for extra-weighting (EW ratio), the spiked initial calibrations were more accurate than the geographically local models. When a 376 377 large number of local samples (32) were considered as spiking subset size (SS = 32), and also as 'n' of the geographically local models (n = 32), scarce differences between 378 both approaches were observed, except for the reduced robustness obtained with the 379 geographically local models (Figure 5). 380

381

#### 382 4. Discussion

#### 383 4.1. Effect of spiking

The predictions obtained using the unspiked initial calibrations had a low accuracy. The 384 bias was the main problem, representing more than 50% of the error, as some authors 385 observed (e.g. Bellon-Maurel & McBratney, 2011). These results were expected, and 386 clearly demonstrate how we cannot safely used calibrations do not cover the 387 characteristics of the target sites. As for any model, the spectroscopic calibrations are 388 valid only for samples with similar characteristics as those used in the calibration 389 (Viscarra Rossel et al., 2008). For these reasons, there is a trend to develop large 390 spectral libraries (Shepherd & Walsh, 2002; Brown et al., 2006; Viscarra Rossel, 2009; 391 392 Grinand et al., 2012; Viscarra Rossel & Webster, 2012). But the accuracy of the calibrations improved drastically when only eight local samples were added to spike the 393 initial calibrations. Once the calibrations contained relevant information for the target 394 site, the predictions became more accurate. The improved accuracy was mostly due to 395 the decrease in bias, in accordance with previous studies (e.g. Stork & Kowalski, 1999; 396 Bricklemyer & Brown, 2010; Guerrero et al., 2010; Stenberg et al., 2010; Wetterlind & 397 398 Stenberg, 2010), but also by an improvement in precision. Many factors affect soil 399 genesis, and soils present an extraordinary variation in composition and characteristics compared with other environmental materials. This makes it difficult to construct a 400 calibration containing the immense variation found in soils, even at a regional scale 401 (Sudduth & Hummel, 1996; Sankey et al., 2008; Minasny et al., 2009; Reeves & Smith, 402 2009). In this way, a large calibration does not guarantee accurate predictions. In fact, 403 several authors observed inaccurate predictions when calibrations were used in samples 404 from independent sites (Christy, 2008; D'Acqui et al., 2010; Wetterlind & Stenberg, 405 2010; Bellon-Maurel & McBratney, 2011). Thus, trying to include all the soil's 406

407 variation is an immense and probably unnecessary effort. Spiking could be an attractive 408 and economical alternative, avoiding the need for large spectral libraries, since we 409 observed the best results when the small-sized initial calibration was spiked. As 410 Guerrero *et al.* (2010) observed, the new information added (i.e. the spiking subset) was 411 more influential on a small-sized initial calibration than on a large-sized one, which 412 explains why better predictions were obtained after spiking the small-sized initial 413 calibration (IC#1).

#### 414 4.2. Effects of extra-weighting on the spiking subset selection strategies

To directly increase the significance or relevance of the added information, several 415 copies of the spiking subset were included in the spiked initial calibrations. The addition 416 of several copies increased their weight and influence on the model (Stork & Kowalski, 417 1999). Under these circumstances, the calibration was forced to fit preferentially to 418 these samples. Consequently, if the extra-weighted samples are representative of the 419 overall prediction set (i.e. the target site), then the calibration must provide reliable 420 predictions for that set. Indeed, extra-weighting caused a significant improvement 421 (P < 0.001) on all the parameters related to the quality of predictions. It is interesting to 422 423 highlight that the effects on the precision (SEP) and accuracy (RMSEP) were similar for 424 the three initial calibrations evaluated, suggesting a robustness of that pattern, since the three initial calibrations were different to each other. So, extra-weighting is a simple, 425 fast and inexpensive task that we recommend when spiking calibrations. The extra-426 weighting caused a strong decrease in the leverage of the spiking subset (Stork & 427 Kowalski, 1999; Capron et al., 2005). Consequently, the extra-weighting could be 428 considered as a manipulation of the spectral space, since it causes a displacement of the 429 calibration centroid toward the extra-weighted samples. In this sense, the extra-430 weighting is a frequent approach used in samples that are added for updating 431

#### **European Journal of Soil Science**

calibrations to new conditions, especially when their number is relatively low in
comparison with the overall calibration set (Stork & Kowalski, 1999), as in our
scenarios (especially in IC#2 and IC#3).

The improvement in the RMSEP, SEP and RPD was dependent on the strategy used 435 to select the spiking subset, as Capron et al. (2005) also observed. The differences 436 found between strategies were similar in the three initial calibrations used, as revealed 437 by the non-significant interaction (P > 0.05) between the 'strategy' and 'initial 438 439 calibration' factors. These results suggest that the effects exerted by the added samples 440 (spiking subset) are not totally controlled by the characteristics of the initial calibration. The soil samples within a local set are different from each other, the information 441 provided by each sample is different (Naes, 1987; Isaksson & Naes, 1990; Shetty et al., 442 2012), and consequently, the improvement in the accuracy of the spiked calibration 443 should also vary. In this sense, using an inadequate spiking subset could be one of the 444 reasons explaining why some authors have found a scarce effect of spiking 445 (Bricklemyer & Brown, 2010; Guerrero et al., 2010). Thus, the identification of a 446 successful strategy to select the most adequate spiking subset is clearly relevant. For 447 these reasons, we evaluated strategies aimed to cover a wide range of different types of 448 spiking subset. Since large bias values have been the most common problem observed 449 450 (Stork & Kowalski, 1999; Janik et al., 2007; Bellon-Maurel & McBratney, 2011), we suspected that using a spiking subset containing strategic SOC values could be adequate 451 452 to improve the bias, and consequently the accuracy. In fact, we observed that the 'OC tails' and 'OC distrib' selection strategies offered better predictions than the 'OC 453 centre', 'OC high' and 'OC low' strategies, since they were adding information in 454 several strategic spaces related with the bias, slope and offset. But it is important to note 455

that the strategies based on the SOC values are not useful in practice, and they wereincluded in the experiment for conceptual evaluation and comparison.

The calibrations spiked with samples evenly distributed in the principal component 458 spectral space ('PC distrib') gave better predictions than those spiked with samples 459 evenly distributed along the concentration values ('OC distrib'). Both strategies select 460 different local samples because the SOC content is not uniquely responsible for the 461 spectral variation within a target site. Compared to texture and mineralogy composition, 462 463 SOC typically has a fairly small influence on spectra (Stenberg et al., 1995; Islam et al., 464 2005; Stenberg et al., 2010). This result is interesting since only the spectral information is available in a real situation (Kusumo et al., 2008; Mora & Schimleck, 465 2008). The predictions obtained with calibrations spiked with a spiking subset selected 466 using the 'PC centre' strategy were less accurate than those selected with 'PC periph'. 467 The samples selected with the 'PC centre' strategy are those more similar to the mean 468 spectrum of the target site. In contrast, those selected with 'PC periph' are more 469 dissimilar to the mean spectrum, but they represent greater diversity. The strategies that 470 included most of the spectral diversity were 'PC distrib' and 'PC periph', and they were 471 two successful strategies, especially the latter. Indeed, there are several methods for 472 optimal sample selection based on spectral characteristics (Naes, 1987; Puchwein, 1988; 473 474 Isaksson & Naes, 1990; Shenk & Westerhaus, 1991; Kusumo et al., 2008) but two of the most commonly used are the Kennard–Stone algorithm (Kennard & Stone, 1969; 475 476 Mora & Schimleck, 2008; Shetty et al., 2012), which covers the experimental region uniformly (as in 'PC distrib'), and the D-optimal procedure (Olsson et al., 2004; 477 Rodionova & Pomerantsev, 2007; Brandmaier et al., 2012), which selects objects 478 located on the periphery (most extreme) of the experimental region (as in 'PC periph'). 479

There were scarce differences between the selections made using the Mahalanobis distance. The values of Mahalanobis distance were extremely high, and all the local samples were always classified as outliers. Consequently, these sets are not sensitive to the Mahalanobis distance criterion. This criterion would probably be relevant when samples from the target sites are more similar to those comprising the initial calibration (Puchwein, 1988; Capron *et al.*, 2005).

486 4.3. Increase of spiking subset size versus extra-weighting, and comparison with
487 geographically local models

488 When the 'PC distrib' strategy was used to select the spiking subset, extra-weighting was preferred over the increase in spiking subset size. This was a very interesting result, 489 since extra-weighting caused a significant improvement inaccuracy without any 490 analytical effort. In contrast, the increase of the spiking subset size implies efforts in 491 terms of time and money, and the improvement of the RMSEP was not statistically 492 significant. The non-significant improvement of the RMSEP was probably due to the 493 high efficiency of the 'PC distrib' strategy to select the most representative samples. 494 Consequently, a further addition of samples would prove scarcely useful, since the new 495 496 added samples would be redundant (in comparison with the first ones selected). These 497 results agree with those obtained by other authors (Naes, 1987; Puchwein, 1988; Isaksson & Næs, 1990; Capron et al., 2005; D'Acqui et al., 2010; Grinand et al., 2012; 498 Shetty *et al.*, 2012), where only a small subset of samples properly selected can offer a 499 similar accuracy than a larger set. In this context, extra-weighting the spiking subset is 500 an efficient approach, which can avoid the need of large-sized spiking subsets. 501

The influence of spiking was greater in the small-sized initial calibrations than in the large-sized ones (Guerrero *et al.*, 2010). When the extra-weighting was made using the same number of copies regardless of the initial calibration size (EW\_24), this

505 pattern was still present, but clearly to a lesser degree. When the extra-weighting was based on the initial calibration to spiking subset ratio (EW ratio), more copies were 506 included in the large-sized initial calibration (IC#3) than in the smaller-sized initial 507 calibrations (IC#1 and IC#2). However, even under these conditions, the results 508 obtained for the three initial calibrations were similar. This result was very interesting 509 because it suggests that small-sized initial calibrations could offer a similar accuracy 510 511 than large-sized initial calibrations. Consequently, this approach can be considered as a 512 strong alternative to the need to develop large spectral libraries. In addition, in those 513 circumstances where only a few local samples can be analysed by the reference method (i.e. 8–16 samples), this approach offered more accurate results than the geographically 514 local (or site-specific) models. When a larger number of local samples were analysed 515 (32 local samples), small differences in accuracy were observed between both 516 approaches, although the geographically local models were less robust, indicating the 517 difficulty to develop consistent spectroscopic calibrations when the number of samples 518 is low. 519

More studies are needed to evaluate if extra-weighting can outperform local models 520 (spectrum-specific models), where a dedicated model is calibrated for an individual 521 unknown sample (Pérez-Marín et al., 2007), or other approaches where a partition of 522 523 the spectral information is used (Viscarra Rossel & Webster, 2012). It is interesting to highlight that local methods (spectrum-specific) can be used only when the spectral 524 525 library contains similar samples to the target site samples, which is not the case for sets evaluated in this paper. In contrast, spiking with a properly selected spiking subset, 526 together with extra-weighting, can overcome this problem, allowing the extrapolation of 527 the initial calibrations applicability. 528

529

#### 530 Conclusions

The addition of a small spiking subset (eight local samples) to spike the calibrations 531 improved the accuracy of the SOC predictions. There were, however, important 532 differences in accuracy, which were dependent on the strategy used to select the spiking 533 534 subset. The best results were obtained when the calibrations were spiked with local samples that were evenly distributed across the space defined by the first three principal 535 536 components (spiking subset selected with the 'PC distrib' strategy). In addition, extraweighting was an effective way to improve the accuracy of the spiked calibrations. 537 Extra-weighting of the spiking subset accentuates the spiking effect, giving an 538 acceptable level of accuracy when predictions of SOC are needed at local scale, and 539 when using small-sized spiking subsets. Large-sized calibrations are probably not 540 needed when these approaches are considered, since similar results were obtained with 541 542 the small- and large-sized calibrations, and it suggests that incipient spectral libraries 543 could be useful if they are properly spiked and extra-weighted. Consequently, extraweighting is a simple, fast and inexpensive task that we highly recommend when 544 calibrations are spiked, and can avoid the need to develop geographically local models. 545 546 Overall, our results indicate that the efforts needed to use NIR spectroscopy for SOC 547 assessment at local scales can be minimised.

#### 548 Acknowledgements

This work was part of a research project (Ref. CGL2011-27001) sponsored by the Spanish Government Ministerio de Economía y Competitividad, and C. Guerrero gratefully acknowledges this financial support. C. Guerrero acknowledges the Spanish Government Ministerio de Educación for a travel grant (ref. JC2011-0342). F.T. Maestre was supported by the European Research Council through the European

- 554 Commission's Seventh Framework Programme (FP7/2007-2013) under grant
- agreement no. 242658 (BIOCOM).

557	References
558	Bellon-Maurel, V. & McBratney, A. 2011. Near-infrared (NIR) and mid-infrared (MIR)
559	spectroscopic techniques for assessing the amount of carbon stock in soils - Critical
560	review and research perspectives. Soil Biology and Biochemistry, 43, 1398-1410.
561	Brandmaier, S., Sahlin, U., Tetko, I.V. & Oberg, T. 2012. PLS-Optimal: A stepwise D-
562	Optimal design based on latent variables. Journal of Chemical Information and
563	Modeling, <b>52</b> , 975–983.
564	Bricklemyer, R.S. & Brown, D.J. 2010. On-the-go VisNIR: Potential and limitations for
565	mapping soil clay and organic carbon. Computers and Electronics in Agriculture,
566	70, 209–216.
567	Brown, D.J. 2007. Using a global VNIR soil-spectral library for local soil
568	characterization and landscape modelling in a 2nd-order Uganda watershed.
569	Geoderma, <b>140</b> , 444–453.
570	Brown, D.J., Bricklemyer, R.S. & Millar, P.R. 2005. Validation requirements for
571	diffuse reflectance soil characterization models with a case study of VNIR soil C
572	prediction in Montana. Geoderma, <b>129</b> , 251–267.
573	Brown, D.J., Shepherd, K.D., Walsh, M.G., Mays, M.D. & Reinsch, T.G. 2006. Global
574	soil characterization with VNIR diffuse reflectance spectroscopy. Geoderma, 132,
575	273–290.
576	Capron, X., Walczak, B., de Noord, O.E. & Massart, D.L. 2005. Selection and
577	weighting of samples in multivariate regression model updating. Chemometrics and

Intelligent Laboratory Systems, 76, 205–214. 578

579	Christy, C.D. 2008. Real-time measurement of soil attributes using on-the-go near
580	infrared reflectance spectroscopy. Computers and Electronics in Agriculture, 61,
581	10–19.
582	D'Acqui, L.P., Pucci, A. & Janik, L.J. 2010. Soil properties prediction of western
583	Mediterranean islands with similar climatic environments by means of mid-infrared
584	diffuse reflectance spectroscopy. European Journal of Soil Science, 61, 865-876.
585	Genot, V., Colinet, G., Bock, L., Vanvyve, D., Reusen, Y. & Dardenne, P. 2011. Near
586	infrared reflectance spectroscopy for estimating soil characteristics valuable in the
587	diagnosis of soil fertility. Journal of Near Infrared Spectroscopy, 19, 117–138.
588	Gogé, F., Joffre, R., Jolivet, C., Ross, I. & Ranjard, L. 2012. Optimization criteria in
589	sample selection step of local regression for quantitative analysis of large soil NIRS
590	database. Chemometrics and Intelligent Laboratory Systems, 110, 168–176.
591	Grinand, C., Barthès, B.G., Brunet, D., Kouakoua, E., Arrouays, D., Jolivet, C., Caria,
592	G. & Bernoux, M. 2012. Prediction of soil organic and inorganic carbon contents at
593	a national scale (France) using mid-infrared reflectance spectroscopy (MIRS).
594	European Journal of Soil Science, <b>63</b> , 141–151.
595	Guerrero, C., Zornoza, R., Gómez, I. & Mataix-Beneyto, J. 2010. Spiking of NIR
596	regional models using simples from target sites: Effect of model size on prediction
597	accuracy. Geoderma, 158, 66–77.
598	Isaksson, T. & Naes, T. 1990. Selection of samples for calibration in near-infrared
599	spectroscopy. Part II: selection based on spectral measurements. Applied
600	<i>Spectroscopy</i> , <b>44</b> , 1152–1158.

#### **European Journal of Soil Science**

601	Islam, K., McBratney, A. & Singh, B. 2005. Rapid estimation of soil variability from
602	the convex hull biplot area of topsoil ultra-violet, visible and near-infrared diffuse
603	reflectance spectra. Geoderma, 128, 249–257.

- Janik, L.J., Skjemstad, J.O., Sheperd, K.D. & Spouncer, L.R. 2007. The prediction of
- soil carbon fractions using mid-infrared-partial least square analysis. *Australian Journal of Soil Research*, 45, 73–81.
- Kennard, R.W. & Stone, L.A. 1969. Computer aided design of experiments.
   *Technometrics*, 11, 137–148.
- 609 Kuang, B. & Mouazen, A.M. 2013. Effect of spiking strategy and ratio on calibration of
- on-line visible and near infrared soil sensor for measurement in European farms. *Soil & tillage Research*, 128, 125–136.
- Kusumo, B.H., Hedley, C.B., Hedley, M.J., Hueni, A., Tuohy, M.P. & Arnold, G.C.
- 613 2008. The use of diffuse reflectance spectroscopy for in situ carbon and nitrogen
  614 analysis of pastoral soils. *Australian Journal of Soil Research*, 46, 623-635.
- 615 Minasny, B., Tranter, A.B., Brough, D.M. & Murphy, B.W. 2009. Regional
- transferability of mid-infrared diffuse reflectance spectroscopic prediction for soil
  chemical properties. *Geoderma*, 153, 155–162.
- Mora, C.R. & Schimleck, L.R. 2008. On the selection of samples for multivariate
  regression analysis: application to near-infrared (NIR) calibration models for the
  prediction of pulp yield in Eucalyptus nitens. *Canadian Journal of Forest Research*,
  38, 2626–2634.
- Naes, T. 1987. The design of calibration in near infrared reflectance analysis by
  clustering. *Journal of Chemometrics*, 1, 121–134.

624	Olsson, I-M., Gottfries, J. & Wold, S. 2004. D-optimal onion designs in statistical
625	molecular design. Chemometrics and Intelligent Laboratory Systems, 73, 37-46.
626	Pérez-Martín, D., Garrido-Varo, A. & Guerrero, J.E. 2007. Non-linear regression
627	method in NIRS quantitative analysis. Talanta, 72, 28–42.
628	Puchwein, G. 1998. Selection of calibration samples for near-infrared spectrometry by
629	factor analysis of spectra. Analytical Chemistry, 60, 569-573.
630	Reeves III, J.B., McCarty, G.W. & Meisinger, J.J. 1999. Near infrared reflectance the
631	analysis of agricultural soils. Journal of Near Infrared Spectroscopy, 7, 179–193.
632	Reeves III, J.B. & Smith, D.B. 2009. The potential of mid- and near-infrared diffuse
633	reflectance spectroscopy for determining major- and trace-element concentrations
634	in soils from a geochemical survey of North America. Applied Geochemistry, 24,
635	1472–1481.
636	Rodionova, O.Y. & Pomerantsev, A.L. 2008. Subset selection strategy. Journal of
637	<i>Chemometrics</i> , <b>22</b> , 674–685.
638	Sankey, J.B., Brown, D.J., Bernard, M.L. & Lawrence, R.L. 2008. Comparing local vs.
639	global visible and near-infared (VisNIR) diffuse reflectance spectroscopy (DRS)
640	calibrations for the prediction of soil clay, organic C and inorganic C. Geoderma,
641	<b>148</b> , 149–158.
642	Shenk, J.S. & Westerhaus, M.O. 1991. Population definition, sample selection, and

- calibration procedures for near-infrared reflectance spectroscopy. Crop Science, 31, 643 644 469–474.
- Shepherd, K.D. & Walsh, M.G. 2002. Development of reflectance spectral libraries for 645 characterization of soil properties. Soil Science Society of America Journal, 66, 646 988–998. 647

### **European Journal of Soil Science**

648	Shetty, N., Rinnan, A. & Gislum, R. 2012. Selection of representative calibration
649	sample sets for near-infrared reflectance spectroscopy for predict nitrogen
650	concentration in grasses. Chemometrics and Intelligent Laboratory Systems, 111,
651	59–65.
652	Stenberg, B., Nordkvist, E. & Salomonsson, L. 1995. Use of near infrared reflectance
653	spectra of soils for objective selection of samples. Soil Science, 159, 109-114.
654	Stenberg, B., Viscarra Rossel, R.A., Mouazen, A.M. & Wetterlind, J. 2010. Visible and
655	near infrared spectroscopy in soil science. Advances in Agronomy, 107, 163–215.
656	Stork, C.L. & Kowalski, B.R. 1999. Weighting schemes for updating regression models
657	- a theoretical approach. Chemometrics and Intelligent Laboratory Systems, 48,
658	151–166.
659	Sudduth, K.A. & Hummel, J.W. 1996. Geographical operating range evaluation of a
660	NIR soil sensor. Transactions of the ASAE, 39, 1599–1604.
661	Viscarra Rossel, R.A. & Webster, R. 2012. Predicting soil properties from the
662	Australian soil visible-near infrared spectroscopic database. European Journal of
663	Soil Science, <b>63</b> , 848–860.
664	Viscarra Rossel, R. 2009. The Soil Spectroscopy Group and the development of a
665	global soil spectral library. NIR News, 20, 14–15.
666	Viscarra Rossel, R.A., Jeon, Y.S., Odeh, I.O.A. & McBratney A.B. 2008. Using a
667	legacy soil sample to develop a mid-IR spectral library. Australian Journal of Soil
668	<i>Research</i> , <b>46</b> , 1–16.
669	Viscarra Rossel, R.A., Cattle, S.R., Ortega, A. & Fouad, Y. 2009. In situ measurements
670	of soil colour, mineral composition and clay content by vis-NIR spectroscopy.
671	<i>Geoderma</i> , <b>150</b> , 253–266.

672	Walkley, A. & Black, I.A. 1934. An examination of the Degtjareff method for
673	determining soil O.M. and a proposed modification of the chromic acid titration
674	method. Soil Science, 37, 29–38.
675	Wetterlind, J. & Stenberg, B. 2010. Near-infrared spectroscopy for within-field soil
676	characterization: small local calibrations compared with national libraries spiked
677	with local samples. European Journal of Soil Science, 61, 823-843.
678	Wetterlind, J., Stenberg, B. & Söderström, M. 2010. Increased sample point density in
679	farm soil mapping by local calibration of visible and near infrared prediction
680	models. <i>Geoderma</i> , <b>156</b> , 152–160.
681	
682	

- 681
- 682

Page 31 of 45

#### 683 FIGURE CAPTIONS

684

**Figure 1** Projections of the NIR spectra from the target sites (TS) into the principal component space defined by the first two principal components, in each initial calibration (IC). Grey stars denote the national samples of the initial calibrations and black dots denote target site samples.

689

Figure 2 Schematic description of the experimental setup: a) initial calibration (IC) 690 691 unspiked, constructed only with national samples (NS); b) initial calibration spiked with a spiking subset (SS) selected by strategy #1; c) initial calibration spiked with spiking 692 subset selected by strategy #1, where an extra-weighting was applied to the spiking 693 subset. This scheme only shows one of the 13 strategies of spiking subset selection and 694 one of the three initial calibrations. This scheme was used with four different target sites 695 (TS). Dashed and double lines denote spiking and the use of the calibration for 696 obtaining predictions  $(\hat{y})$ , respectively. 697

698

**Figure 3a** Representative illustration of predictions obtained in each target site (TS) with the different calibrations conducted. Left: predictions obtained with the unspiked IC#1 (white stars; dotted line). Centre: predictions obtained with IC#1 spiked with the spiking subset selected with the 'MD centre' strategy (white circles, dashed line) and spiking subset extra-weighted (EW) (black circles, solid line). Right: predictions obtained with IC#1 spiked with the spiking subset selected with the 'PC distrib' strategy (white circles, dashed line) and spiking subset extra-weighted (black circles, solid line).

**Figure 3b** Representative illustration of predictions obtained in each target site (TS) with the different calibrations conducted. Left: predictions obtained with the unspiked IC#2 (white stars; dotted line). Centre: predictions obtained with IC#2 spiked with the spiking subset selected with the 'MD centre' strategy (white circles, dashed line) and spiking subset extra-weighted (EW) (black circles, solid line). Right: predictions obtained with IC#2 spiked with the spiking subset selected with the 'PC distrib' strategy (white circles, dashed line) and spiking subset extra-weighted (black circles, solid line).

714

**Figure 3c** Representative illustration of predictions obtained in each target site (TS) with the different calibrations conducted. Left: predictions obtained with the unspiked IC#3 (white stars; dotted line). Centre: predictions obtained with IC#3 spiked with the spiking subset selected with the 'MD centre' strategy (white circles, dashed line) and spiking subset extra-weighted (EW) (black circles, solid line). Right: predictions obtained with IC#3 spiked with the spiking subset selected with the 'PC distrib' strategy (white circles, dashed line) and spiking subset extra-weighted (black circles, solid line).

722

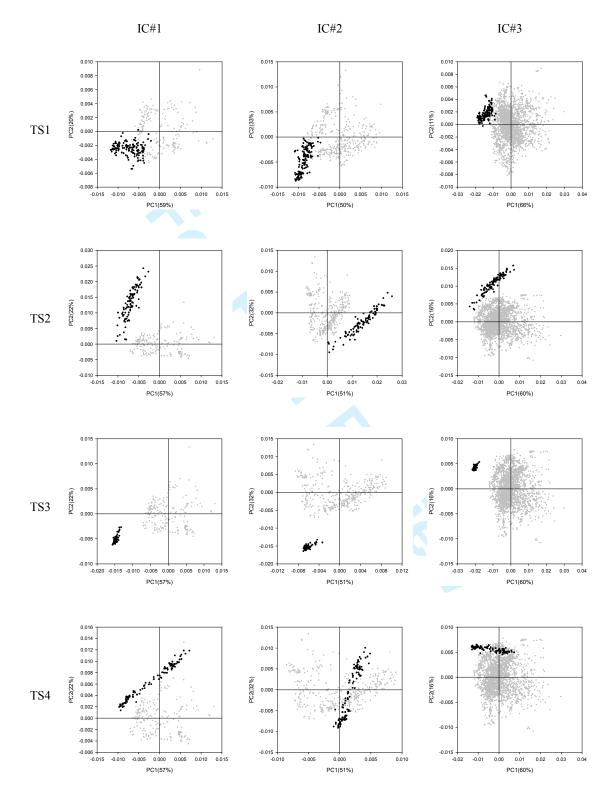
Figure 4 Predictions obtained with unspiked and spiked calibrations (without and with extra-weight) using the 13 different strategies to select the spiking subset. Strategies in spiked calibrations (with and without extra-weighting) are arranged by RMSEP. a) IC#1; b) IC#2; c) IC#3. In all cases, n = 4 (from the four target sites studied). The two horizontal dark grey lines are displaying values of RMSEP = 0.4% soil organic carbon (SOC) and RMSEP = 0.8% SOC to facilitate visual comparisons.

729

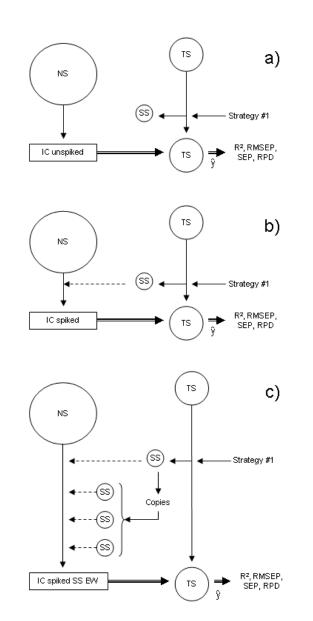
731 Figure 5 Values of the root mean square error of prediction (RMSEP) obtained with the three initial calibrations (IC) spiked with a spiking subset (SS) of size 8 (SS8), 16 732 (SS16) and 32 (SS32), without extra-weight (black bars), and with extra-weight (EW; 733 grey bars). Dark-grey bars are used when 24 copies of the spiking subset were added for 734 extra-weighting (EW 24), and light-grey bars are used when the numbers of copies 735 were added in proportion of the initial calibration to spiking subset ratio (EW ratio). 736 737 White bars and horizontal lines were used to show the RMSEP obtained with 738 geographically local models, constructed uniquely with 8 (horizontal dotted line), 16 739 (horizontal dashed line) or 32 local samples (horizontal solid line). In all the cases, the local samples were selected by the 'PC distrib' strategy. In all the cases n = 4 (from four 740 target sites). The error bars are denoting one standard deviation. 741

- 742
- 743

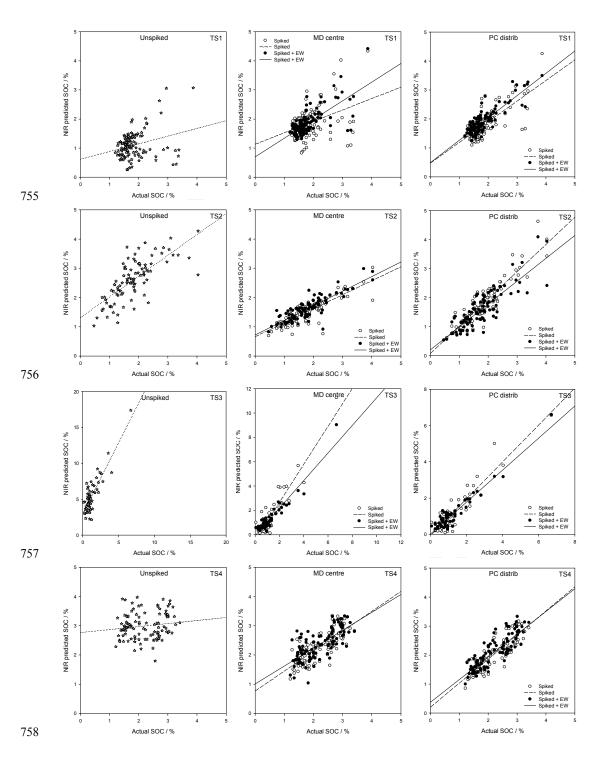


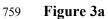


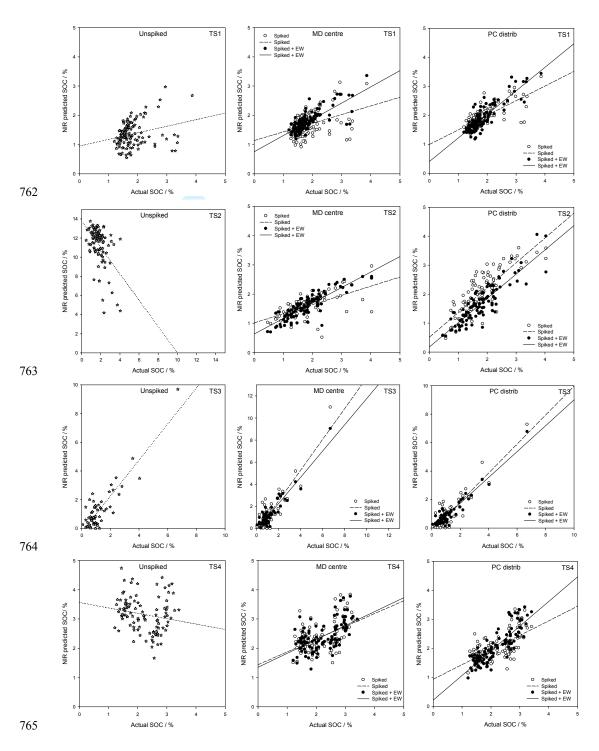
745 **Figure 1** 

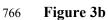


### **Figure 2**

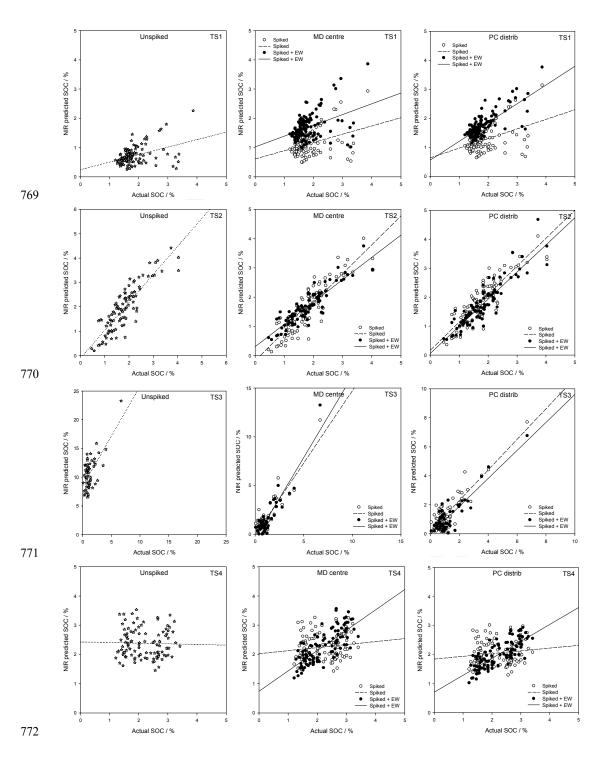




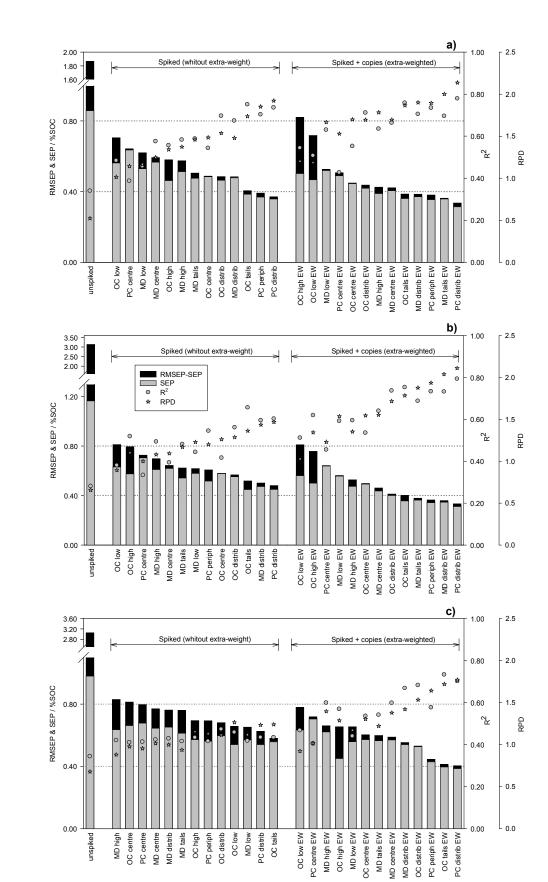




767

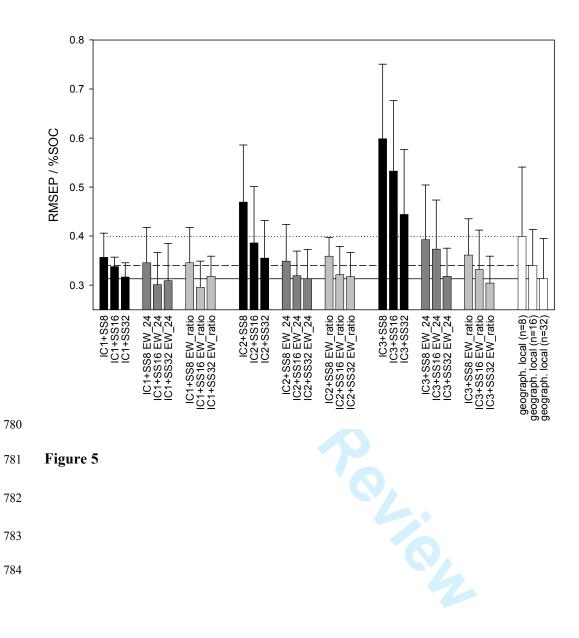






776





#### 785 TABLES

786

**Table 1** Characteristics of the three subsets used for the development of the different Initial

Calibrations (ICs), and the coefficient of determination  $(R^2)$  and root mean square error (RMSE)

obtained in the cross-validations (RMSECV). All the results refer to soil organic carbon (in %).

790

	IC #1	IC #2	IC #3
n	192	365	2279
Minimum	0.32	0.32	0.10
Maximum	8.97	14.49	14.62
Mean	2.35	5.07	1.54
Standard deviation	1.87	3.59	2.14
Skewness	1.05	0.41	3.20
$R^2$	0.95	0.96	0.93
RMSECV	0.40	0.67	0.54

791

**Table 2** Characteristics of the four target sites used. Data refer in all cases to soil organic carbon (SOC; %).

	Target site 1	Target site 2	Target site 3	Target site 4	
Coordinates	55°41'N, 13°19'E	38°32'N, 0°49'W	37°09'N, 2°35'W	52°00'N, 0°26'W	
Site (country)	Sjöstorp (Sweden)	Sax (Spain)	Gergal (Spain)	Silsoe (UK)	
Parent material	Sandy till (25%) and	Gypsum	Mica schists	Mudstone	
	sedimentary clay with				
	elements of chalk (75%)				
Method SOC	LOI <sup>a</sup> (900°C)	Elemental Analyser	Walkley & Black	LOI (900°C)	
Spectral range / nm	1000-2500	834-2650	834-2650	834-2650	
n	125	95	60	104	
Minimum	1.20	0.47	0.07	1.21	
Maximum	3.87	4.04	6.70	3.41	
Mean	1.83	1.80	1.23	2.20	
Standard deviation	0.50	0.71	1.05	0.60	
<sup>a</sup> LOI: loss on ignition					

798 Table 3 Results of the repeated measures ANOVA to evaluate the effects of extra-weighting, initial calibration and strategy on the different prediction

- performance parameters: root mean square error of prediction (RMSEP), standard error of prediction (SEP) and ratio of performance to deviance (RPD).
- 800

Variable		Source	Sum of squares	Degrees of freedom	Mean square	F	Р
RMSEP <sup>a</sup>	Between-subjects	Initial Calibration (IC)	0.605	2	0.302	11.84	0.0000
	Between-subjects	Strategy	0.701	7	0.100	3.918	0.0011
	Between-subjects	IC × Strategy	0.078	14	0.005	0.220	0.9985
	Between-subjects	Error	1.840	72	0.025		
	Within-subjects	Extra-weighting (EW)	0.668	1	0.668	81.90	0.0000
	Within-subjects	EW×IC	0.015	2	0.007	0.956	0.3890
	Within-subjects	$EW \times Strategy$	0.045	7	0.006	0.794	0.5940
	Within-subjects	$EW \times IC \times Strategy$	0.085	14	0.006	0.751	0.7165
	Within-subjects	Error (EW)	0.587	72	0.008		
SEP <sup>b</sup>	Between-subjects	IC	1.872	2	0.936	6.593	0.0023
	Between-subjects	Strategy	3.760	7	0.537	3.782	0.0015
	Between-subjects	$IC \times Strategy$	0.420	14	0.030	0.211	0.9988
	Between-subjects	Error	10.22	72	0.142		
	Within-subjects	EW	2.125	1	2.125	60.76	0.0000
	Within-subjects	$EW \times IC$	0.126	2	0.063	1.801	0.1725
	Within-subjects	$EW \times Strategy$	0.235	7	0.033	0.959	0.4673
	Within-subjects	$EW \times IC \times Strategy$	0.306	14	0.021	0.626	0.8346
	Within-subjects	Error (EW)	2.518	72	0.035		
RPD <sup>♭</sup>	Between-subjects	IC	3.209	2	1.604	7.372	0.0012
	Between-subjects	Strategy	3.716	7	0.531	2.439	0.0266
	Between-subjects	$IC \times Strategy$	0.417	14	0.029	0.137	0.9999
	Between-subjects	Error	15.67	72	0.217		
	Within-subjects	EW	3.543	1	3.543	81.90	0.0000
	Within-subjects	$EW \times IC$	0.082	2	0.041	0.956	0.3890
	Within-subjects	EW × Strategy	0.240	7	0.034	0.794	0.5940
	Within-subjects	EW × IC × Strategy	0.454	14	0.032	0.751	0.7165
	Within-subjects	Error (EW)	3.114	72	0.043		

801 <sup>a</sup> Log transformed

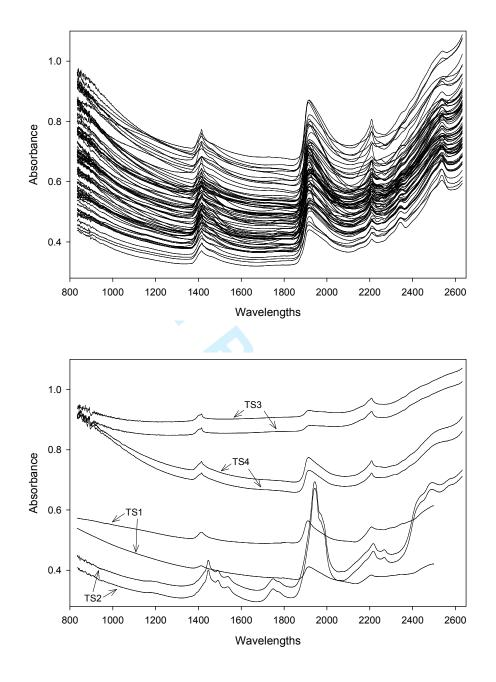
802 <sup>b</sup> Ln transformed

Table 4. Results of the repeated measures ANOVAs to evaluate the effects of the spiking subset size (SS-size), and those of the extra-weighting (EW) on the
root mean square error of prediction (RMSEP) obtained with spiked calibrations. (a) Results obtained when 24 copies where used for EW (EW\_24). (b)
Results obtained when the number of copies to add for EW was equal to the ratio between the IC size and the SS size (EW\_ratio).

|--|

		Source	Sum of squares	Degrees of freedom	Mean square	F	Р
(a)	Between-subjects	SS-size	0.0696	2	0.0348	2.328	0.1133
	Between-subjects	Error	0.4936	33	0.0149		
	Within-subjects	EW_24	0.1341	1	0.1341	21.28	0.0000
	Within-subjects	$EW_{24} \times SS$ -size	0.0087	2	0.0043	0.695	0.5058
	Within-subjects	Error	0.2079	33	0.0063		
(b)	Between-subjects	SS-size	0.0649	2	0.0324	3.117	0.0575
	Between-subjects	Error	0.3437	33	0.0104		
	Within-subjects	EW_ratio	0.1578	1	0.1578	18.45	0.0001
	Within-subjects	$EW\_ratio \times SS\text{-size}$	0.0119	2	0.0059	0.695	0.5058
	Within-subjects	Error	0.2821	33	0.0085		

808



Supplementary content: **Appendix I.** Representative NIR spectra of the national samples included in the initial calibrations (top), and two representative NIR spectra of each of the four target sites (bottom).

CERES https://dspace.lib.cranfield.ac.uk

School of Aerospace, Transport and Manufacturing (SATM)

2014-01-17

## Assessment of soil organic carbon at local scale with spiked NIR calibrations: effects of selection and extra-weighting on the spiking subset

### Guerrero, C.

Wiley

Guerrero, C. et al. (2014) Assessment of soil organic carbon at local scale with spiked NIR calibrations: effects of selection and extra-weighting on the spiking subset. European Journal of Soil Science, Volume 65, Issue 2, pp. 248-263 http://dx.doi.org/10.1111/ejss.12129 Downloaded from Cranfield Library Services E-Repository